

Supplementary Information

Two Cyclotrimeratrylene Metal-Organic Frameworks as Effective Catalysts for Knoevenagel Condensation and CO₂ Cycloaddition with Epoxides

Da-Wei Kang,^{a, b} Xue Han,^a Xin-Jun Ma,^b Ying-Ying Liu,^{*a} and Jian-Fang Ma^{*a}

^a *Key Lab of Polyoxometalate Science, Department of Chemistry, Northeast Normal University, Changchun 130024, China*

^b *Inner Mongolia Key Lab of Chemistry of Natural Products and Synthesis of Functional Molecules, College of Chemistry and Chemical Engineering, Inner Mongolia University for the Nationalities, Tongliao, 028000, China.*

* Correspondence authors

E-mail: liuyy147@nenu.edu.cn (Y.-Y. Liu)

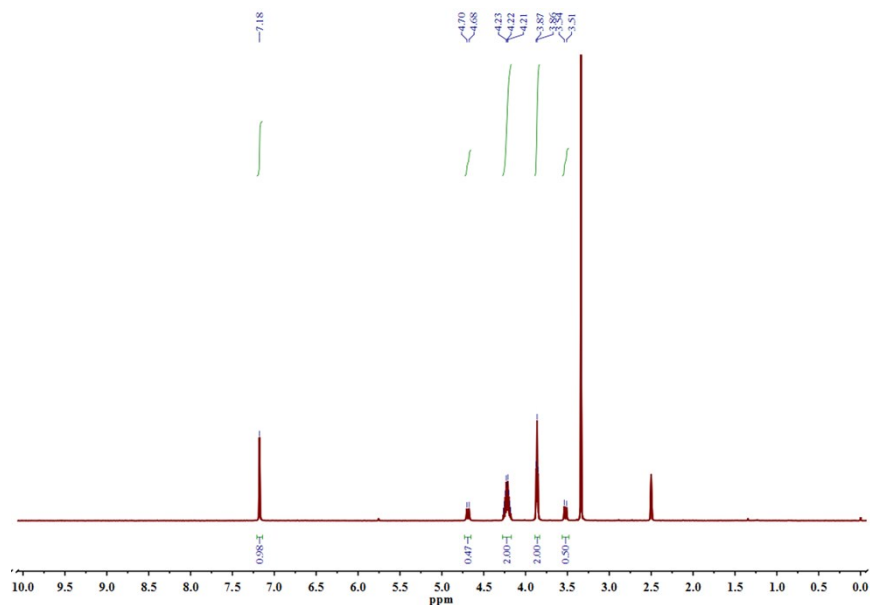
E-mail: majf247@nenu.edu.cn (J.-F. Ma)

Fax: +86-431-85098620 (J.-F. Ma)

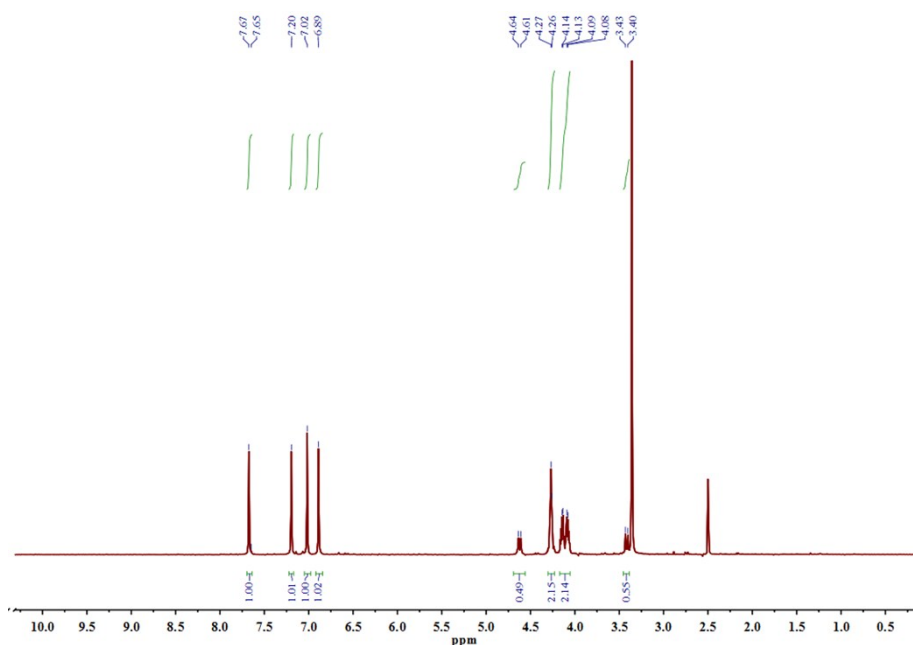
Reagents and Instruments. All chemical reagents and solvents were commercially available. The C, H and N elemental analyses were carried out with a Perkin-Elmer 240C elemental analyzer. (TG) measurements were performed on a Perkin-Elmer TG-7 analyzer, heating from 30 to 1000 °C at a rate of 5 °C min⁻¹ under nitrogen gas. The solid-state emission/excitation spectra were collected with a FLSP920 Edinburgh fluorescence spectrometer. PXRD patterns were recorded on a Rigaku Dmax 2000 X-ray diffractometer with graphite monochromatized Cu K α radiation ($\lambda = 0.154$ nm). ¹H NMR spectra were recorded on a Varian 500 MHz. The catalytic products were measured by gas chromatograph equipment with capillary (30 m long \times 0.25 mm i.d., WondaCAP 17), and FID detector (GC-2014C, Shimadzu, Japan).

X-ray crystallography. Crystallographic data of **1**, **2** and **1a** were determined on an Oxford diffraction Gemini R CCD diffractometer with graphite-monochromated MoK α radiation ($\lambda = 0.71073$ Å) at room temperature. Absorption correction was performed by a

multi-scan technique. The structure was solved by direct methods with SHELXS-97 and refined on F^2 by full-matrix least-squares using the SHELXTL-2014 program within WINGX. Non-hydrogen atoms were refined anisotropically. Hydrogen atoms on carbon were generated geometrically. Crystallographic data, structure refinements, bond distances and angles are given in Tables S1 and S2.



(a)



(b)

Fig. S1 ^1H NMR spectra of intermediate ligand C (a) and final ligand HECTV (b) as shown in Scheme 1.

During the refinements of **1** and **2**, the SQUEEZE routine in PLATON was employed because of the highly disordered solvents. The lattice molecules were demonstrated by the difference Fourier maps of original X-ray data, TGA data (Fig. S2) and elemental analyses.

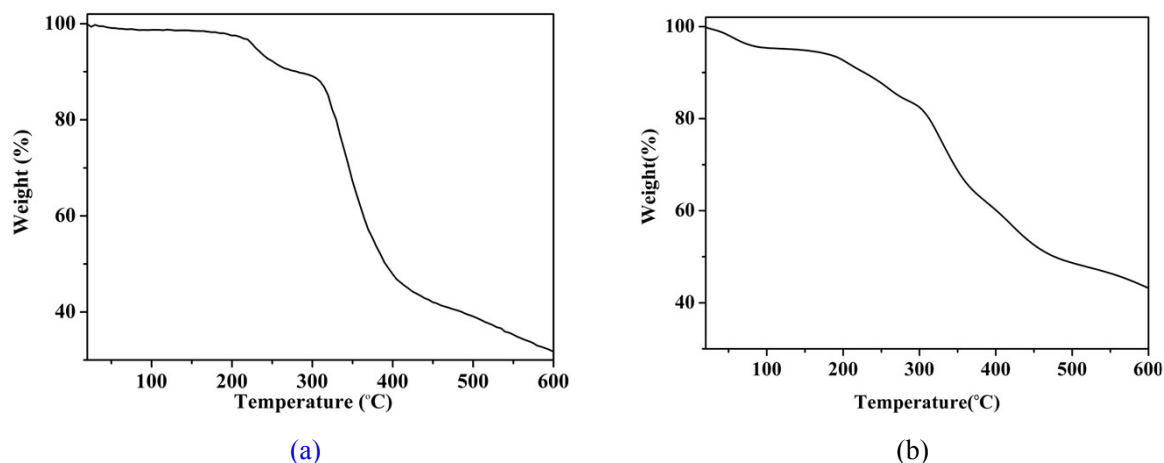


Fig. S2 Thermogravimetric curves of **1** (a) and **2** (b).

For **1**, the weight loss from 35 °C to 263 °C corresponds to the water molecules and DMF molecules (found: 9.42%, calcd: 9.31%). For **2**, the weight loss from 35 °C to 270 °C corresponds to the water molecules and DMF molecules (found: 14.58%, calcd: 14.45%).

Knoevenagel Condensation Reactions. In a typical procedure, aldehyde (1 mmol), malononitrile (1.2 mmol), and **1** (0.005 mmol, 10 mg) were placed in a 10 mL round-bottom flask. Then the mixture was heated to 60 °C and stirred for 1 h. The yields were determined by GC and ¹H NMR spectra with tridecane as internal standard.

Cycloaddition of CO₂ to epoxides. In a typical procedure, epoxide (10 mmol), *n*-Bu₄NBr (32 mg, 0.1 mmol) and **2** (10 mg, 0.005 mmol) were placed in a 10 mL reactor. The reactor was purged several times with CO₂ and bubbled with 1 atm CO₂. Then, the reactor was heated to 80 °C and stirred for 4 h. The product structure was confirmed by ¹H NMR and the yields were calculated by and GC and ¹H NMR .

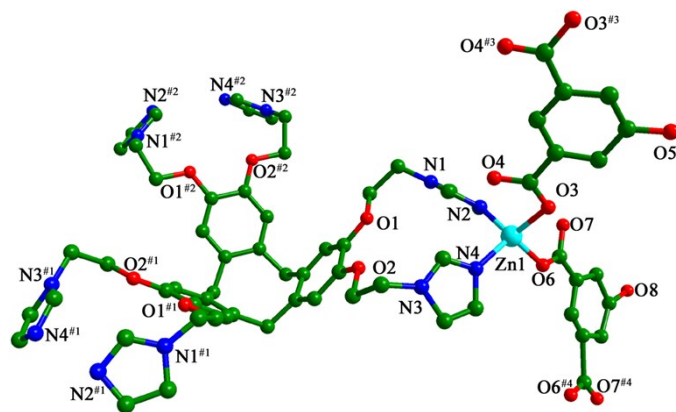


Fig. S3 View of the coordination environment of the Zn(II) cation in **2**. Symmetric codes: #1 - $x+y+1, -x+1, z$; #2 - $-y+1, x-y, z$; #3 $x, y, -z+1/2$; #4 $y+1, x-1, -z$.

To confirm the porosity in the MOFs, we took the typical **1** as an example. The crystals of **1** were immersed in methanol, ethanol and acetone for three days, respectively. Then, thermal analysis was carried out on these samples. They showed obvious profiles characterized by solvent losses (Fig. S4).

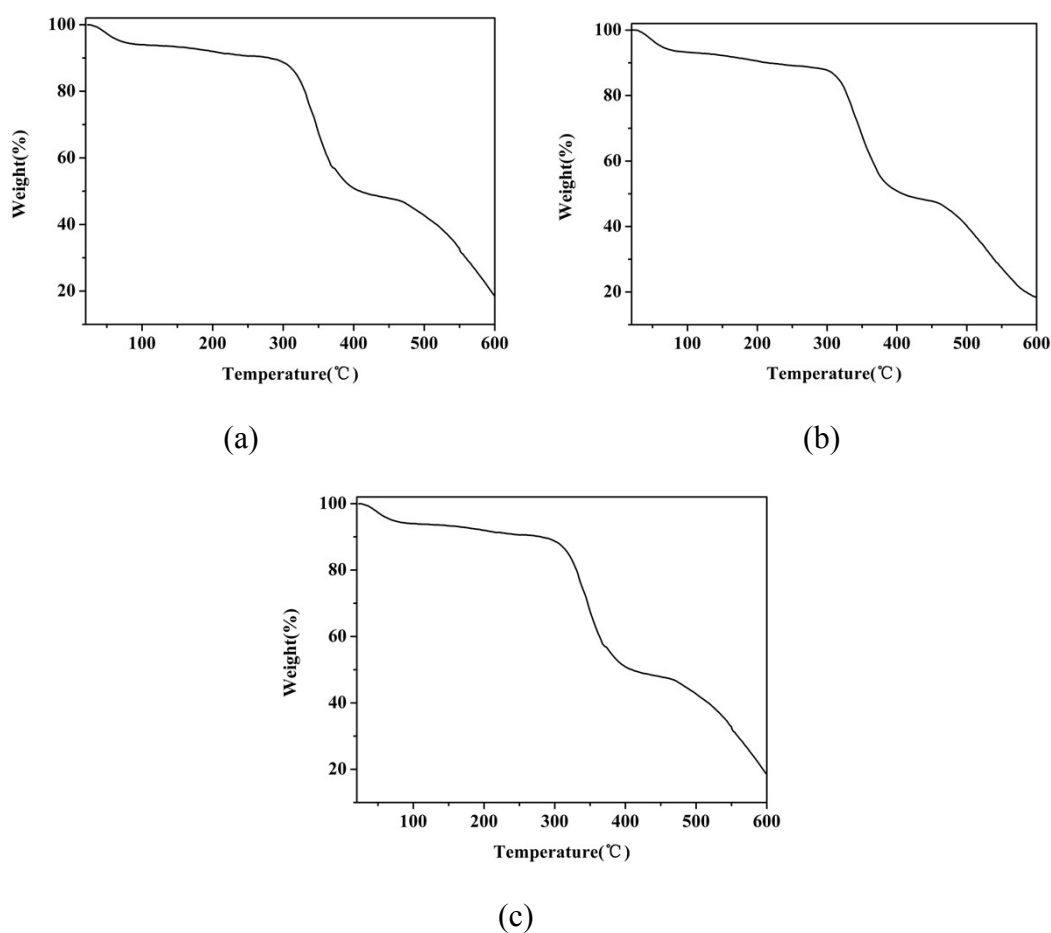
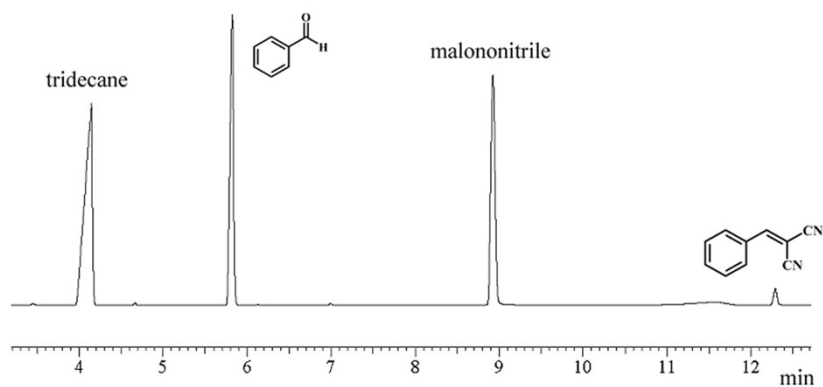
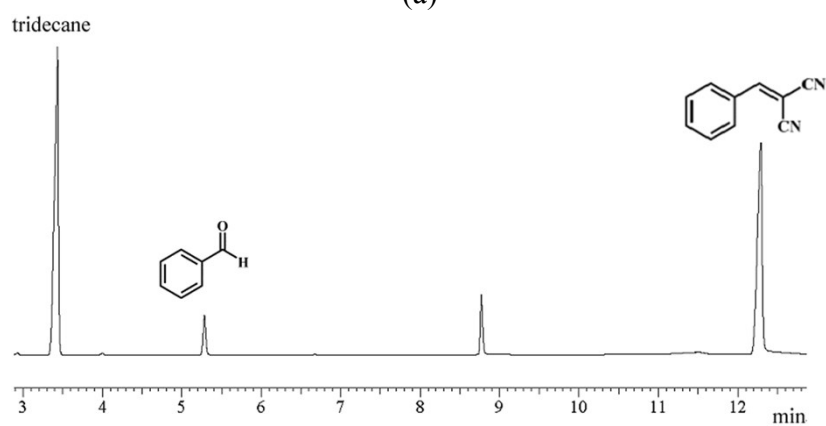


Fig. S4 Thermogravimetric curves of **1** with loading guest molecules of methanol (a), ethanol (b) and acetone (c).

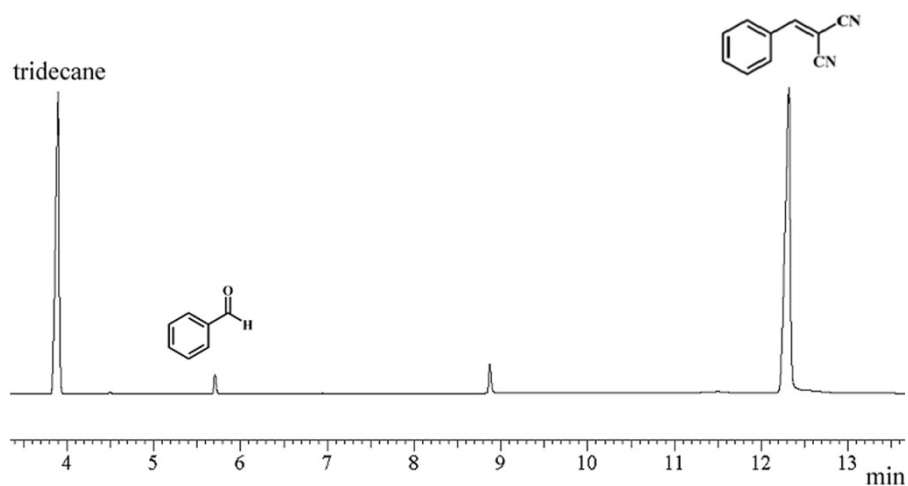
TGA curves exhibit weight losses of ca. 8.1%, 7.5% and 7.4% (in the temperature ranges of 20–120 °C, 20–130 °C and 20–100 °C), which are ascribed to the release of methanol, ethanol and acetone, respectively.



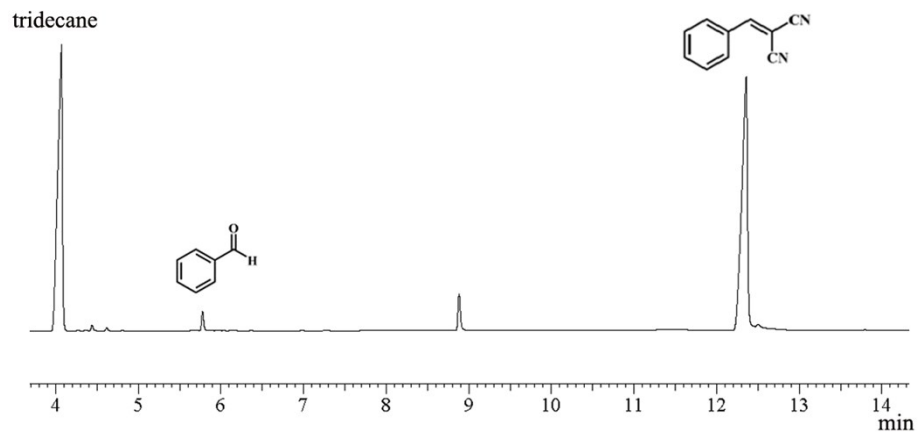
(a)



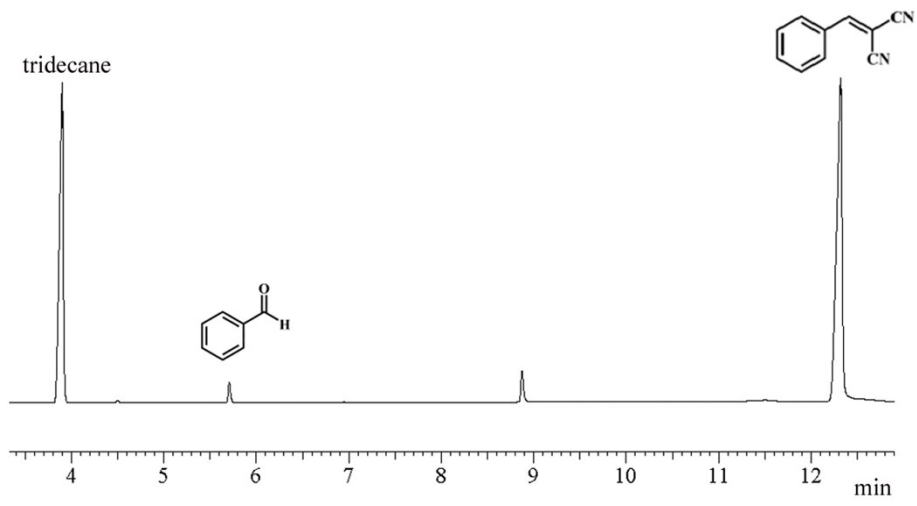
(b)



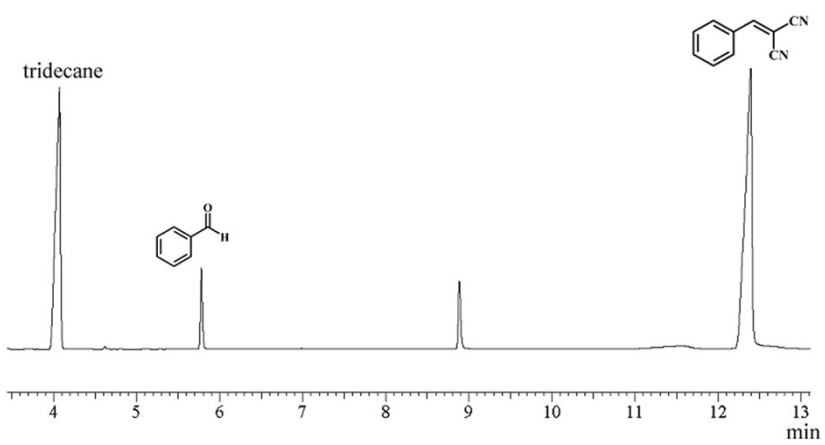
(c)



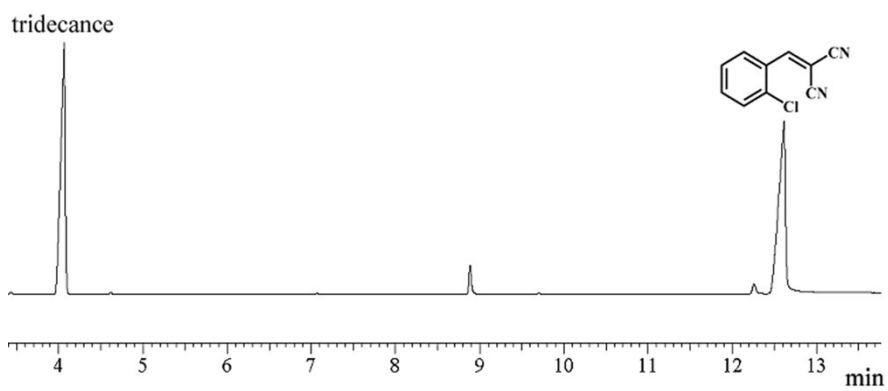
(d)



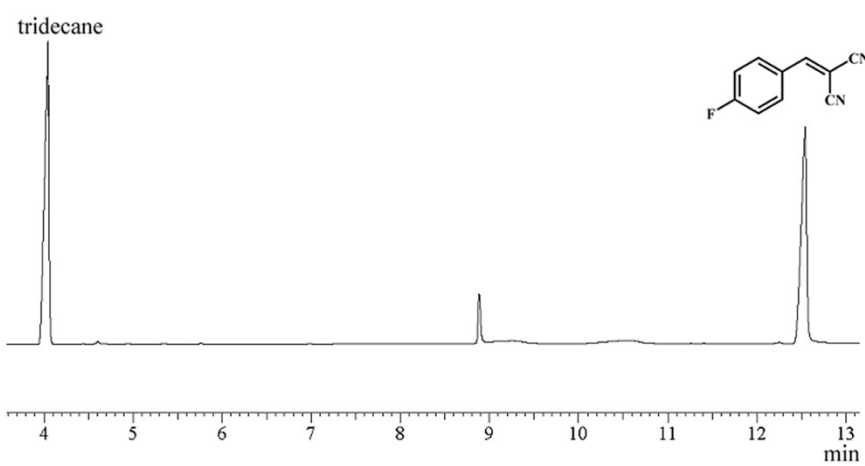
(e)



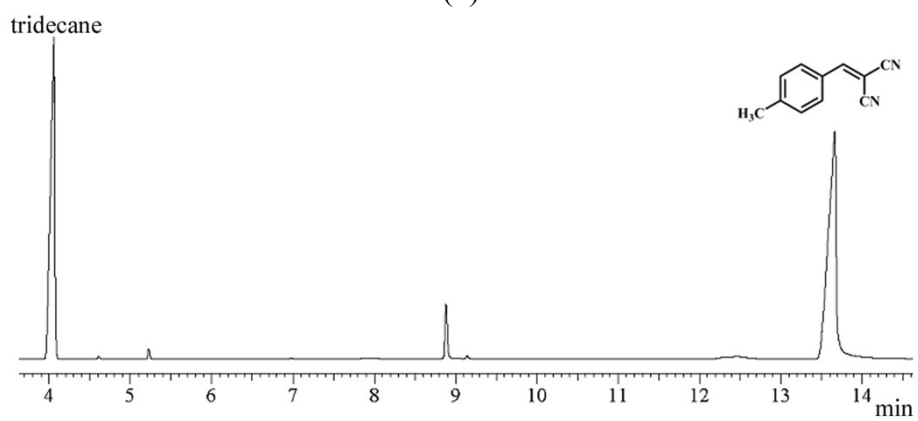
(f)



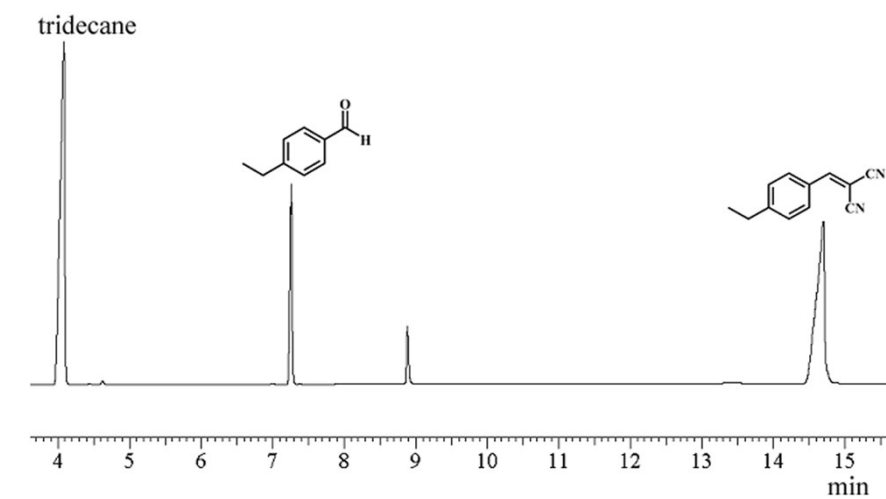
(g)



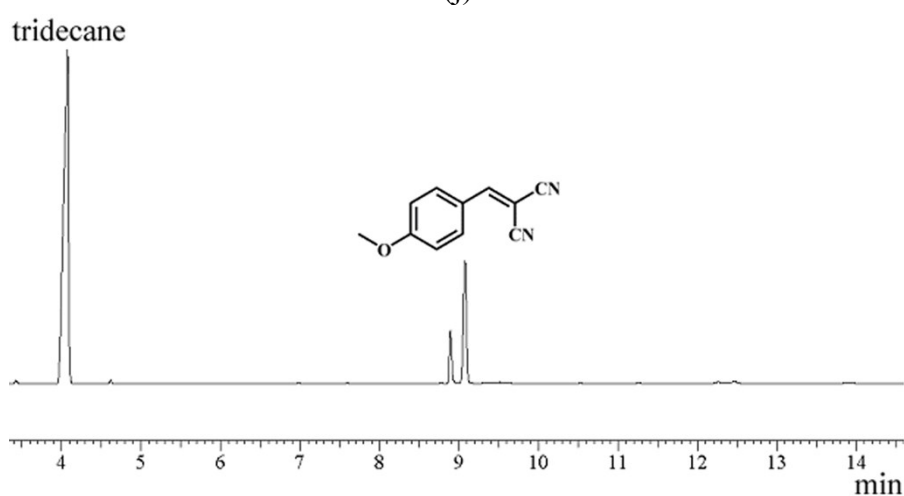
(h)



(i)



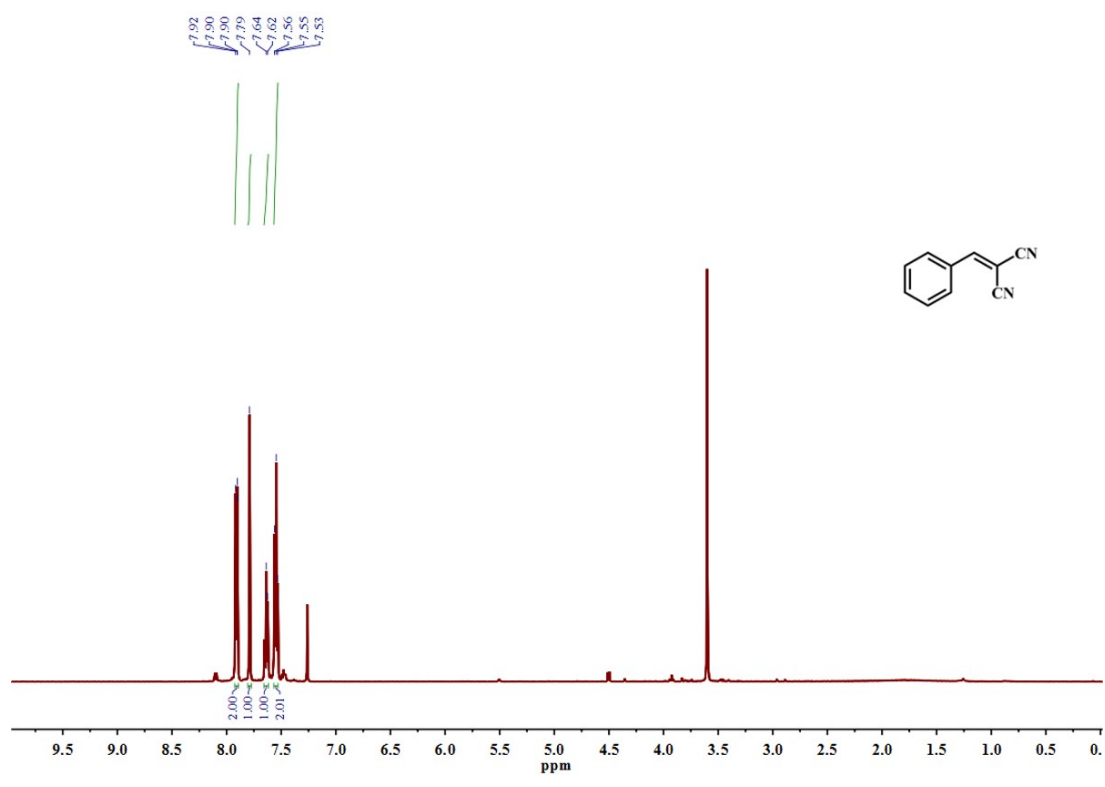
(j)



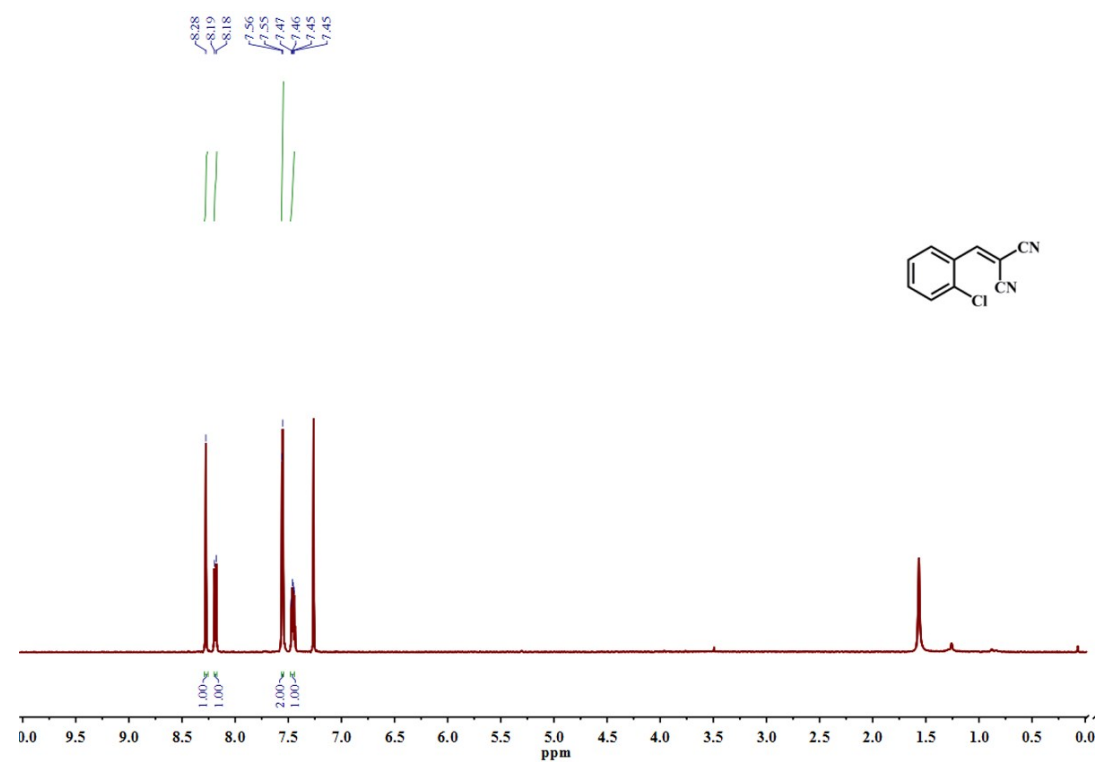
(k)

Fig. S5 GC of Knoevenagel condensation reaction of malononitrile.

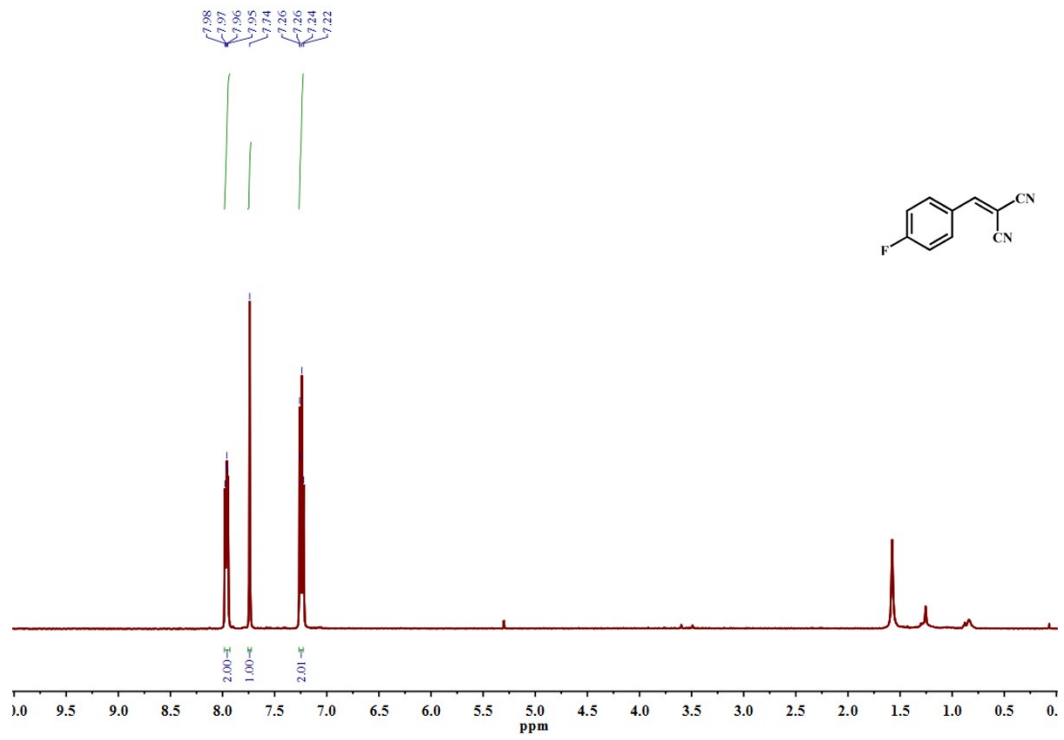
- (a) With benzaldehyde without catalyst after 60 mins.
- (b) With benzaldehyde using catalyst **1** after 30 mins.
- (c) With benzaldehyde using catalyst **1** after 60 mins.
- (d) With benzaldehyde using catalyst **2** after 60 mins.
- (e) With benzaldehyde using catalyst **1a** after 60 mins.
- (f) With benzaldehyde using catalyst $\text{Cd}(\text{NO}_3)_2 \cdot 4\text{H}_2\text{O}$ after 60 mins.
- (g) With 2-chlorobenzaldehyde using catalyst **1** after 60 mins.
- (h) With 4-fluorobenzaldehyde using catalyst **1** after 60 mins.
- (i) With 4-methylbenzaldehyde using catalyst **1** after 60 mins.
- (j) With 4-ethylbenzaldehyde using catalyst **1** after 60 mins.
- (k) With 4-methoxybenzaldehyde using catalyst **1** after 60 mins.



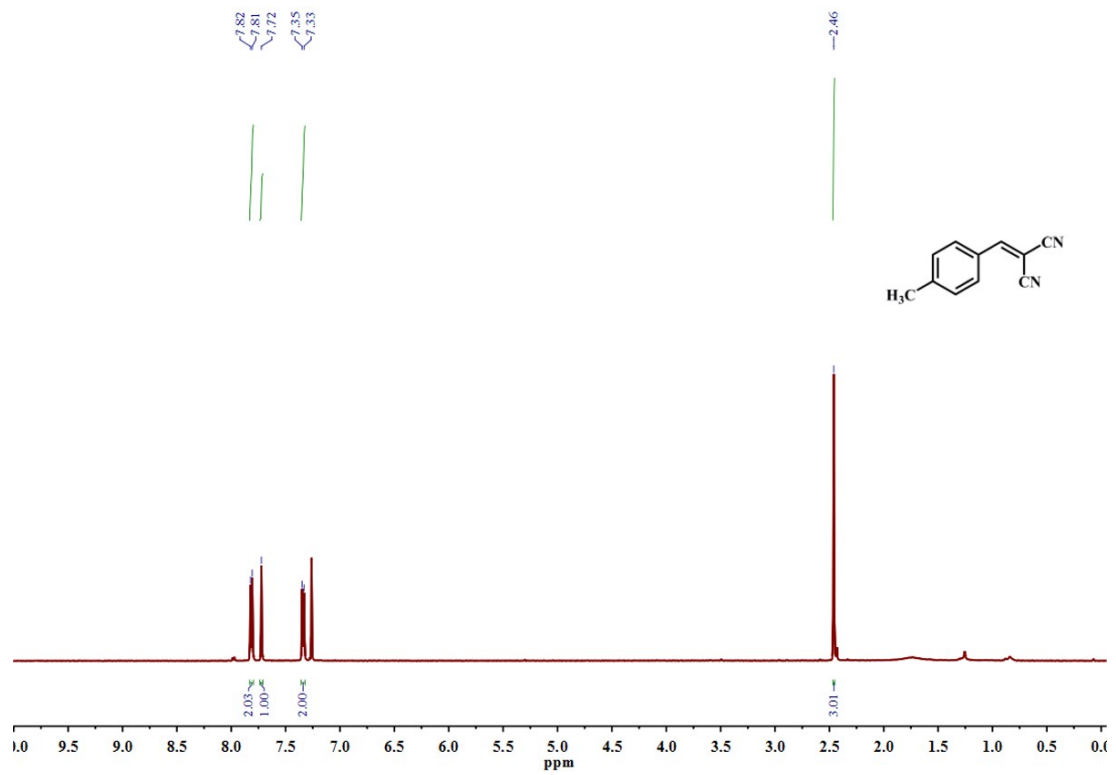
(a)



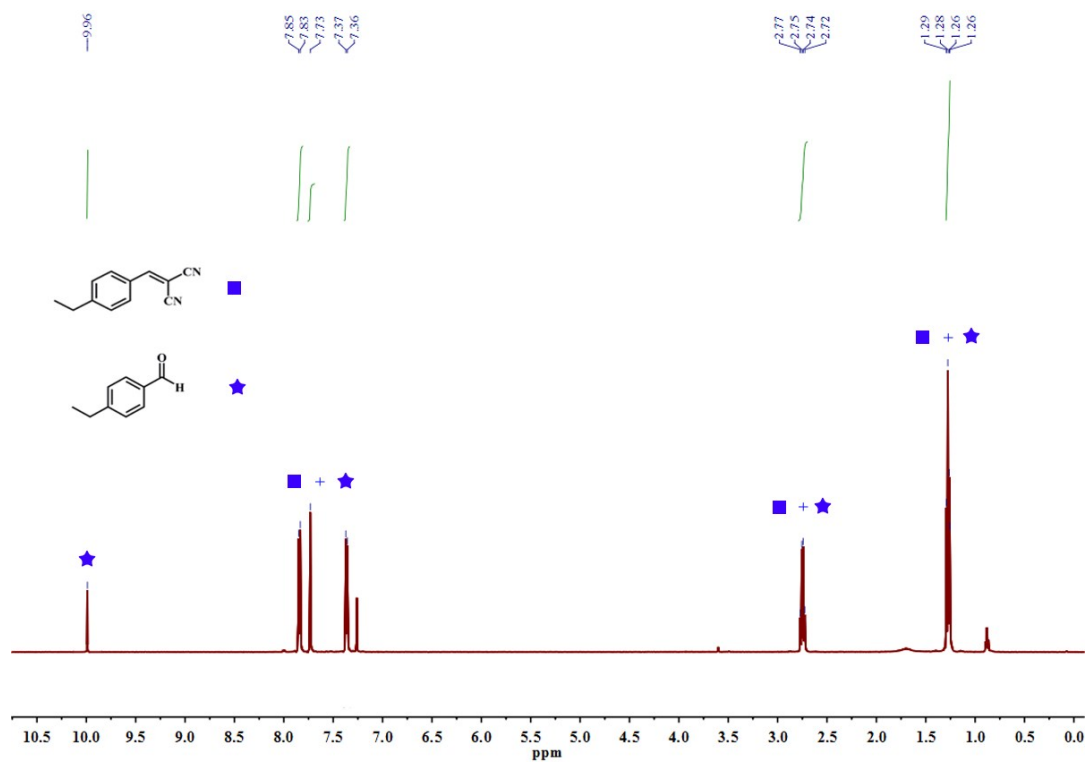
(b)



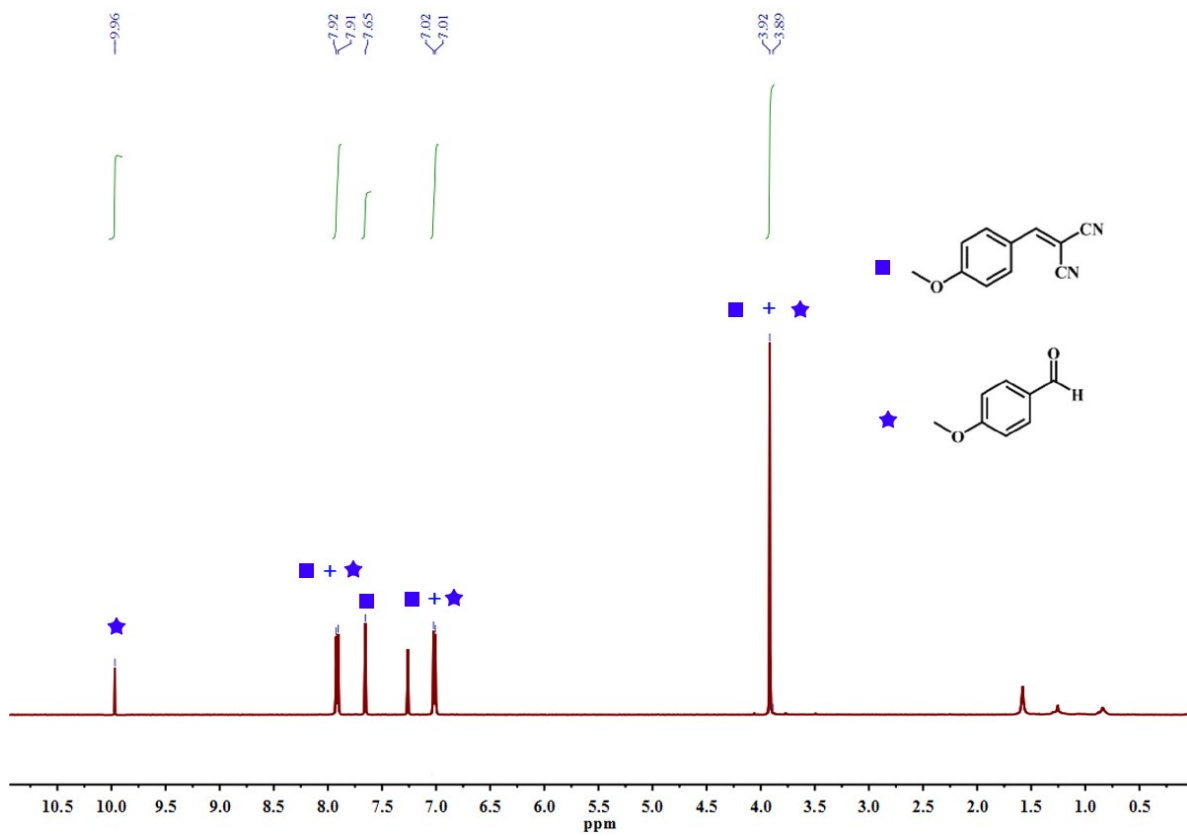
(c)



(d)



(e)



(f)

Fig. S6 ^1H NMR spectrum of the crude products from the Knoevenagel condensation reaction of malononitrile with (a) Benzaldehyde. (b) 2-Chlorobenzaldehyde. (c) 4-Fluorobenzaldehyde. (d) 4-Methylbenzaldehyde. (e) 4-Ethylbenzaldehyde. (f) 4-Methoxybenzaldehyde.

The signals in the range of 0.5-2.0 ppm maybe caused by the catalytic internal standard tridecane. The signal at 5.3 ppm is caused by the impurity CH_2Cl_2 in CDCl_3 during the ^1H NMR testing.

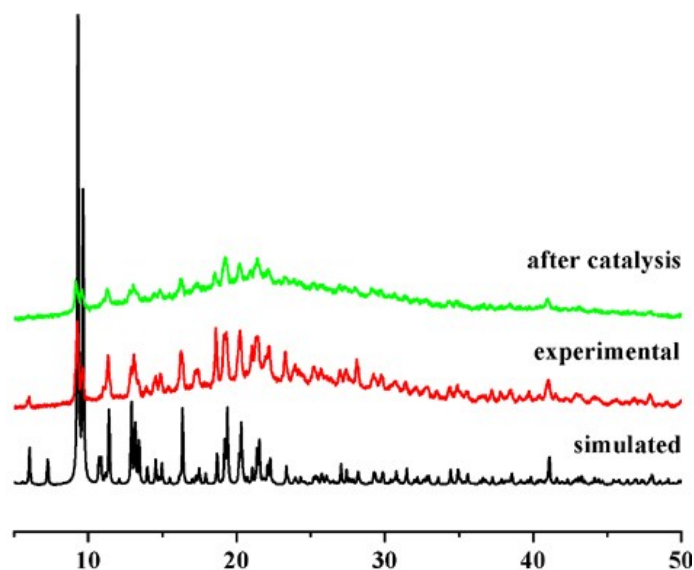
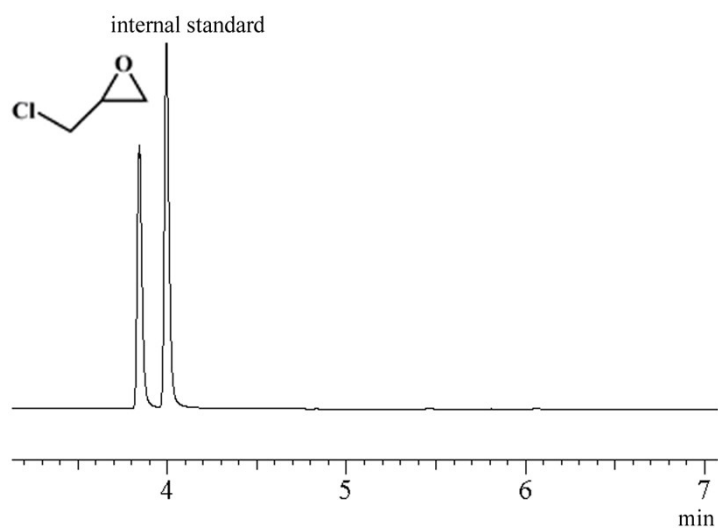
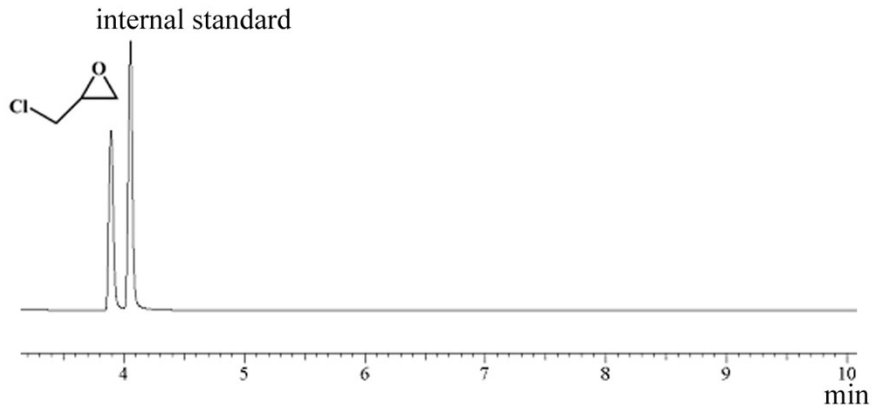


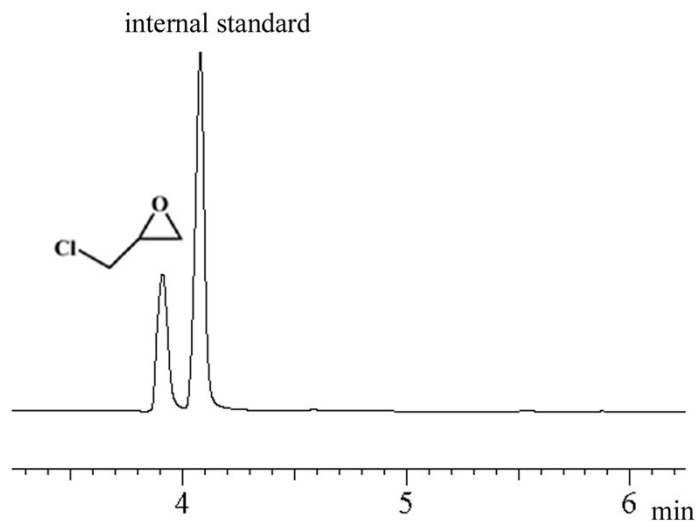
Fig. S7 PXR D patterns of **1** simulated (black), the experimental (red) and after 4 cycles Knoevenagel condensation reaction (green).



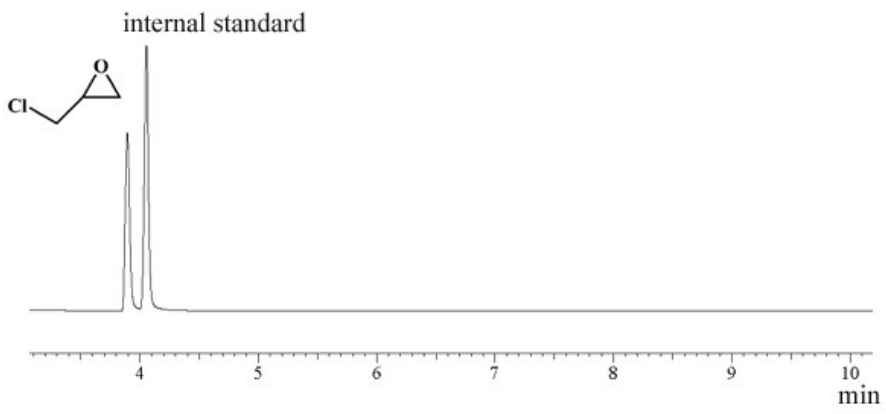
(a)



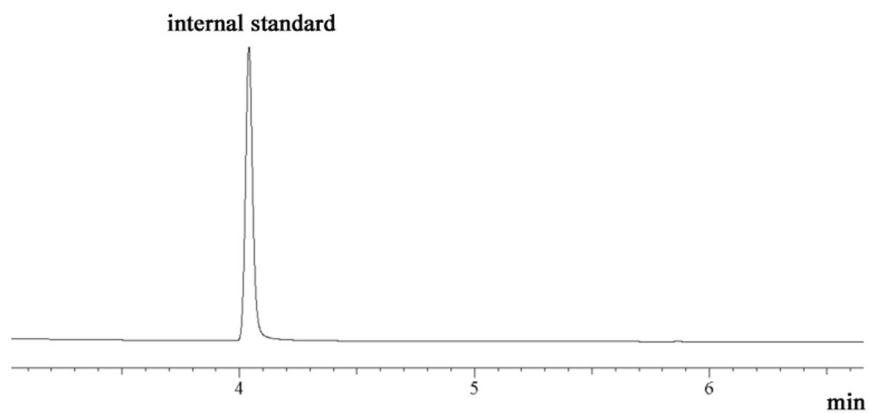
(b)



(c)

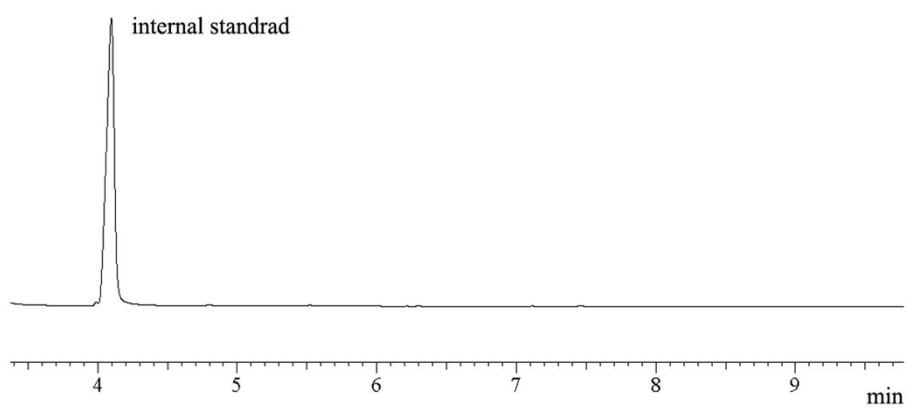


(d)

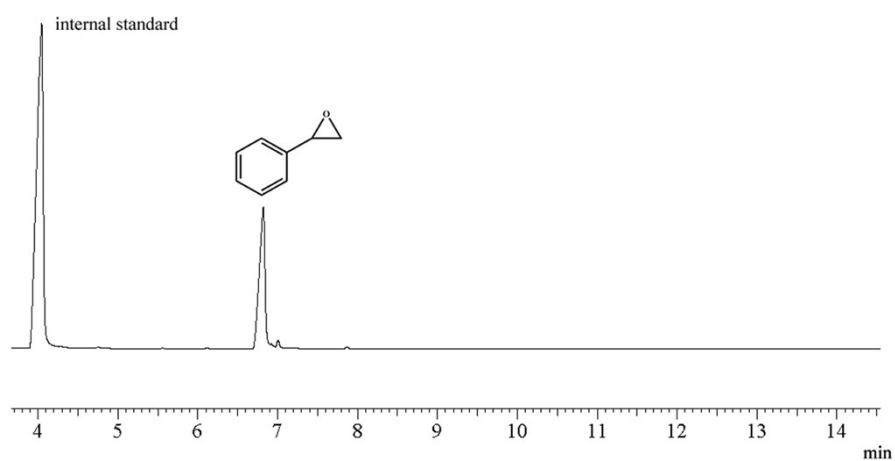


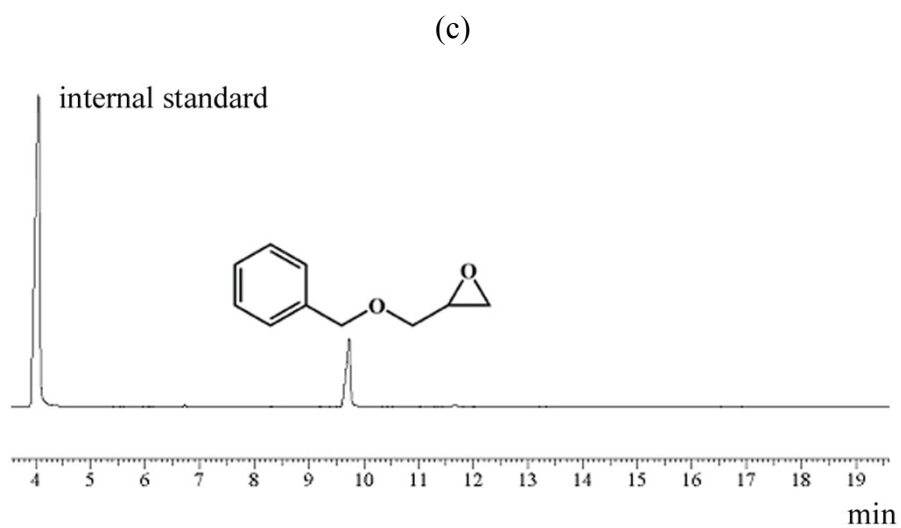
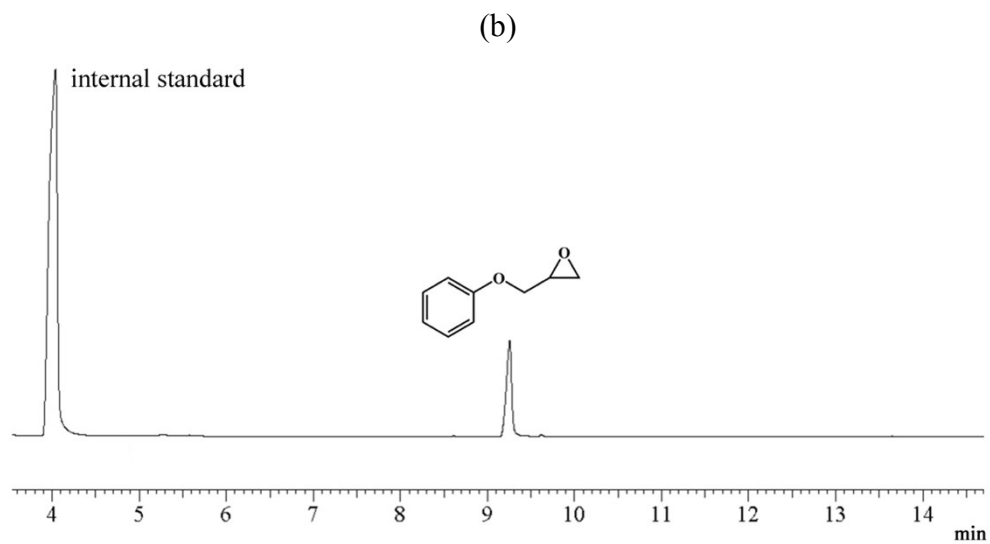
(e)

Fig. S8 GC of cycloaddition of CO₂ to epichlorohydrin using (a) Catalyst **1** for 2 hours at 1 atm. (b) *n*-Bu₄NBr as catalyst for 2 hours at 1 atm. (c) Catalyst **1** and *n*-Bu₄NBr as co-catalyst for 2 hours at 1 atm. (d) Catalyst **2** for 2 hours at 1 atm. (e) Catalyst **2** and *n*-Bu₄NBr as co-catalyst for 2 hours at 1 atm.



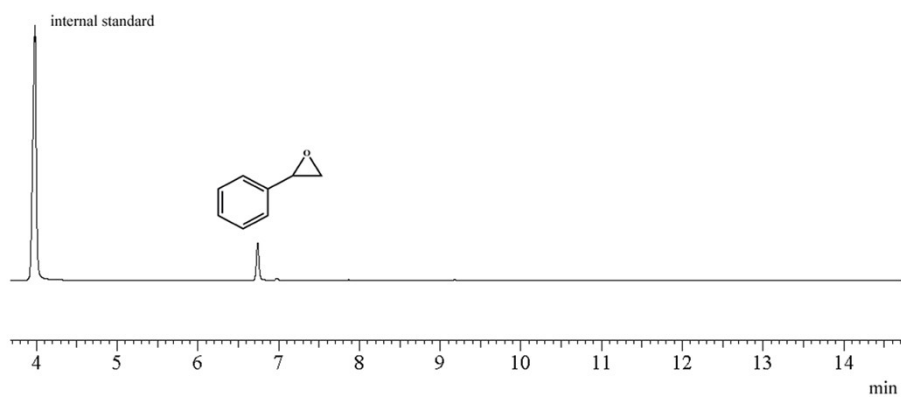
(a)



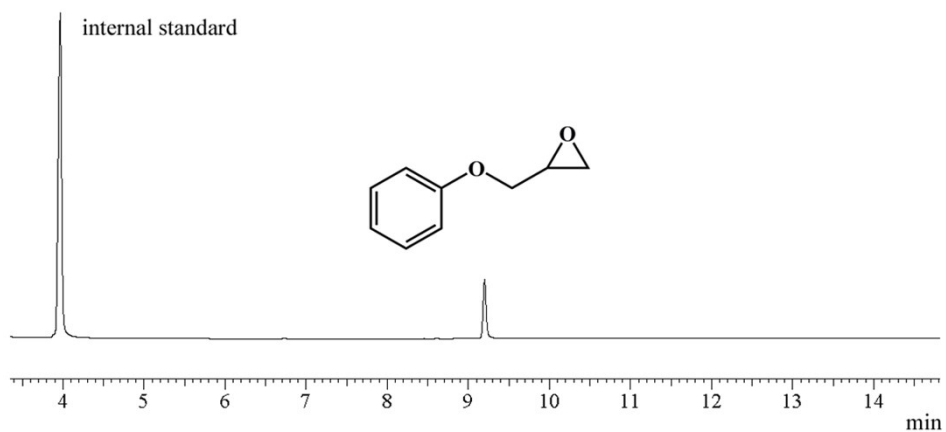


(d)

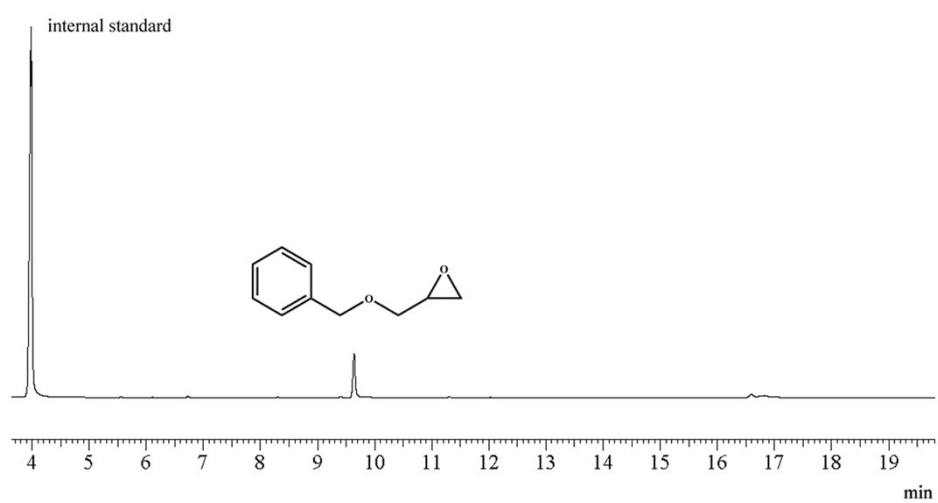
Fig. S9 GC of cycloaddition of CO₂ to (a) 1,2-Epoxyhexane using catalyst **2** and *n*-Bu₄NBr as co-catalyst for 2 hours. (b) 1,2-Epoxyethylbenzene (c) Glycidyl phenyl ether (d) Benzylglycidylether using catalyst **2** and *n*-Bu₄NBr as co-catalyst for 4 hours.



(a)

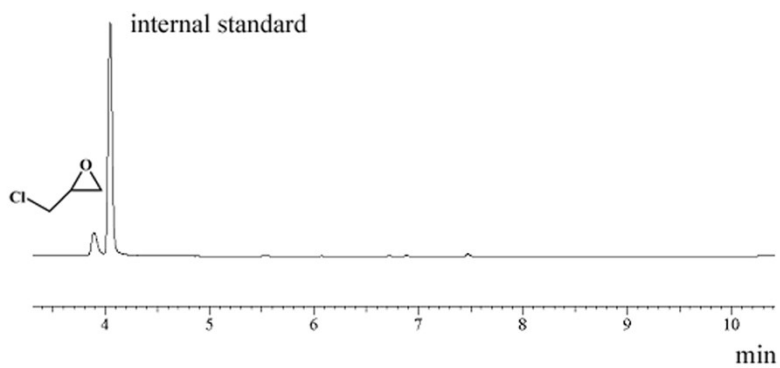


(b)

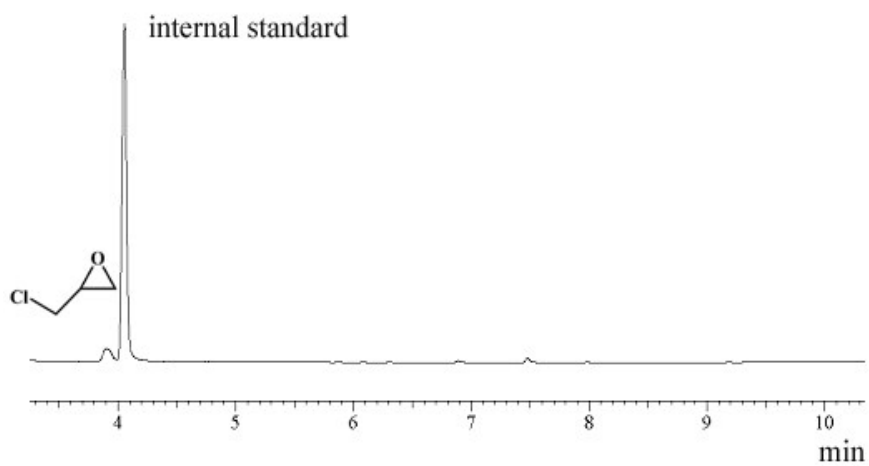


(c)

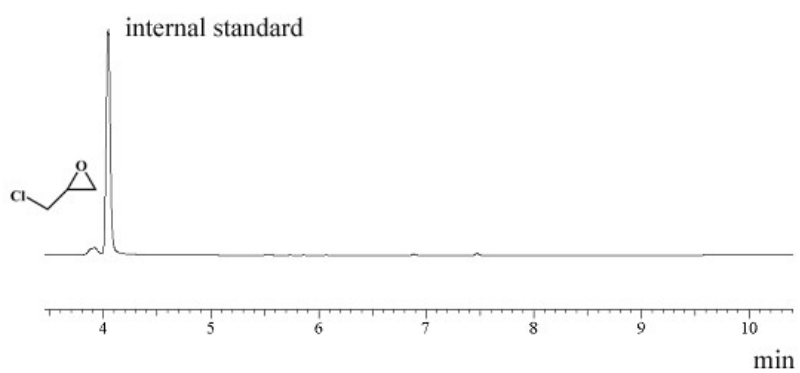
Fig. S10 GC of cycloaddition of CO₂ to (a) 1,2-Epoxyethylbenzene (b) Glycidylphenylether (c) Benzylglycidylether using catalyst **2** and *n*-Bu₄NBr as co-catalyst for 12 hours.



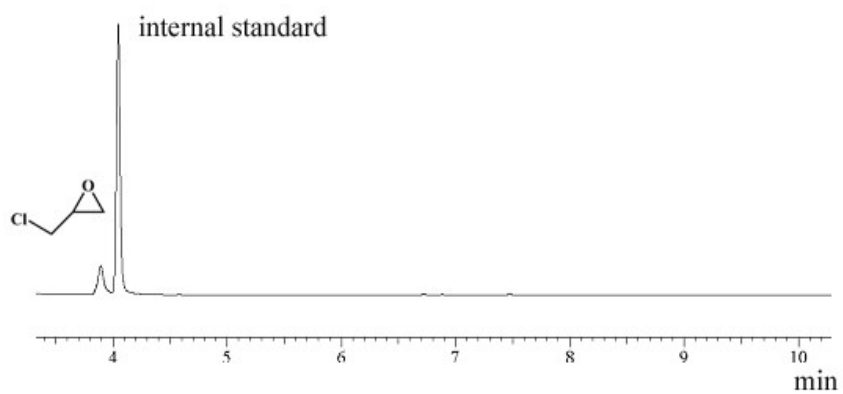
(a)



(b)

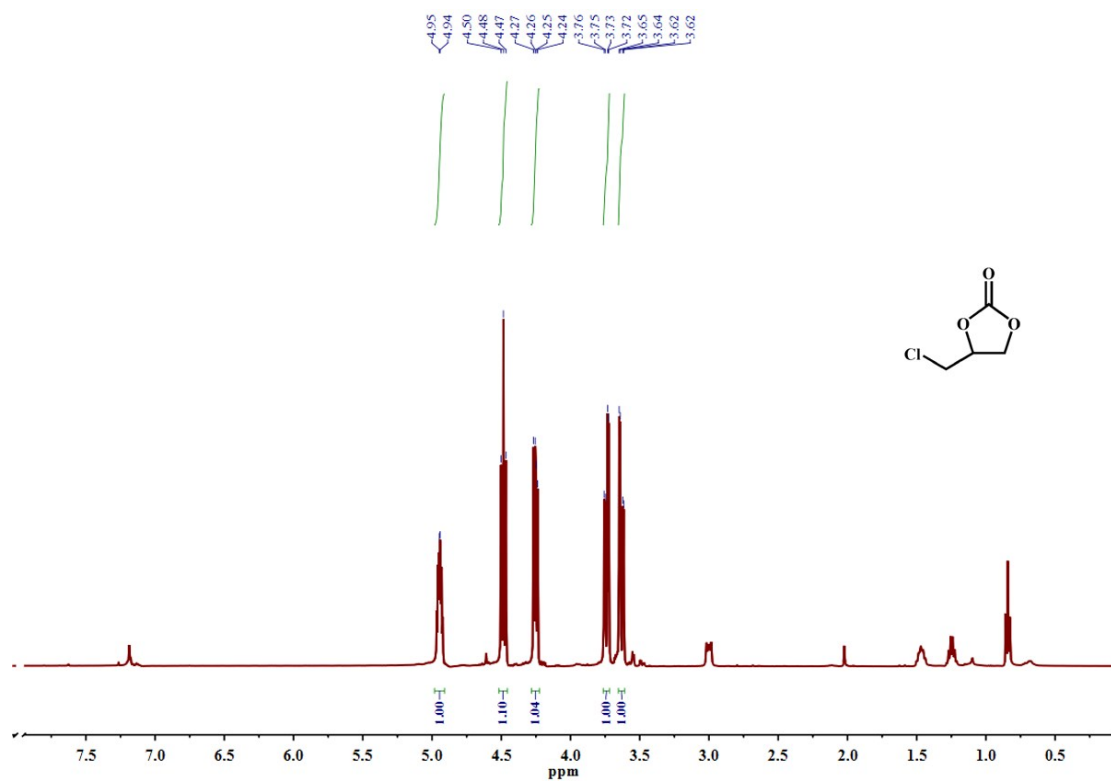


(c)

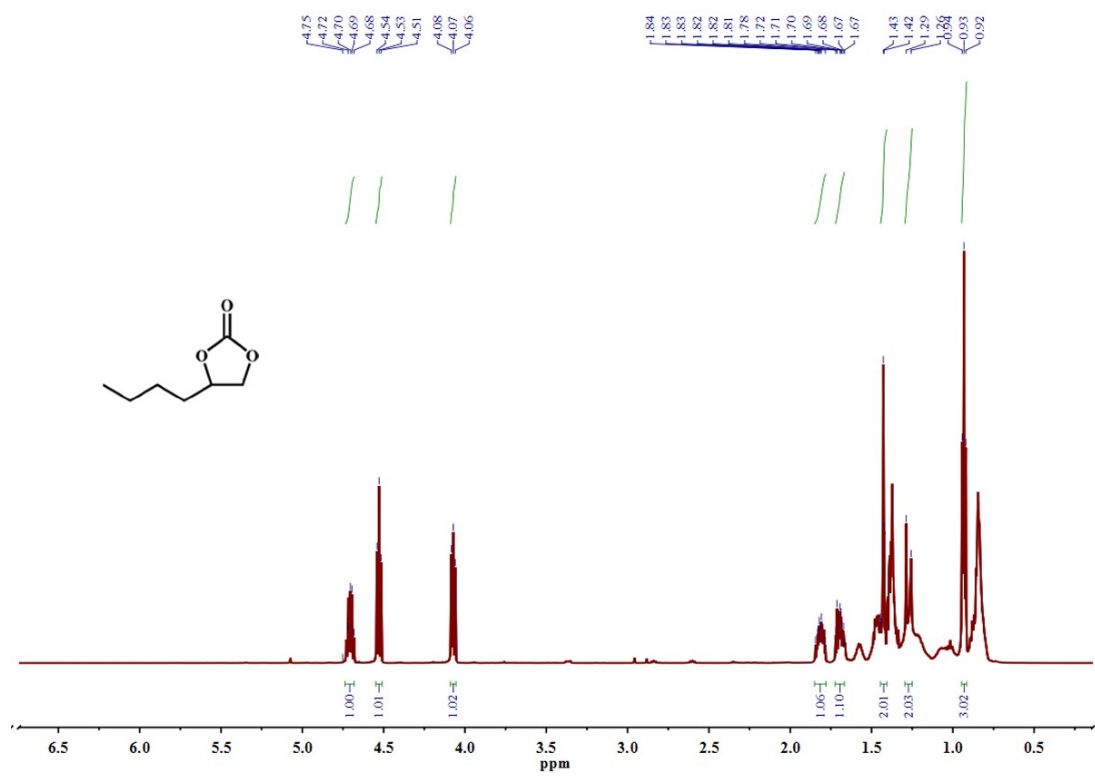


(d)

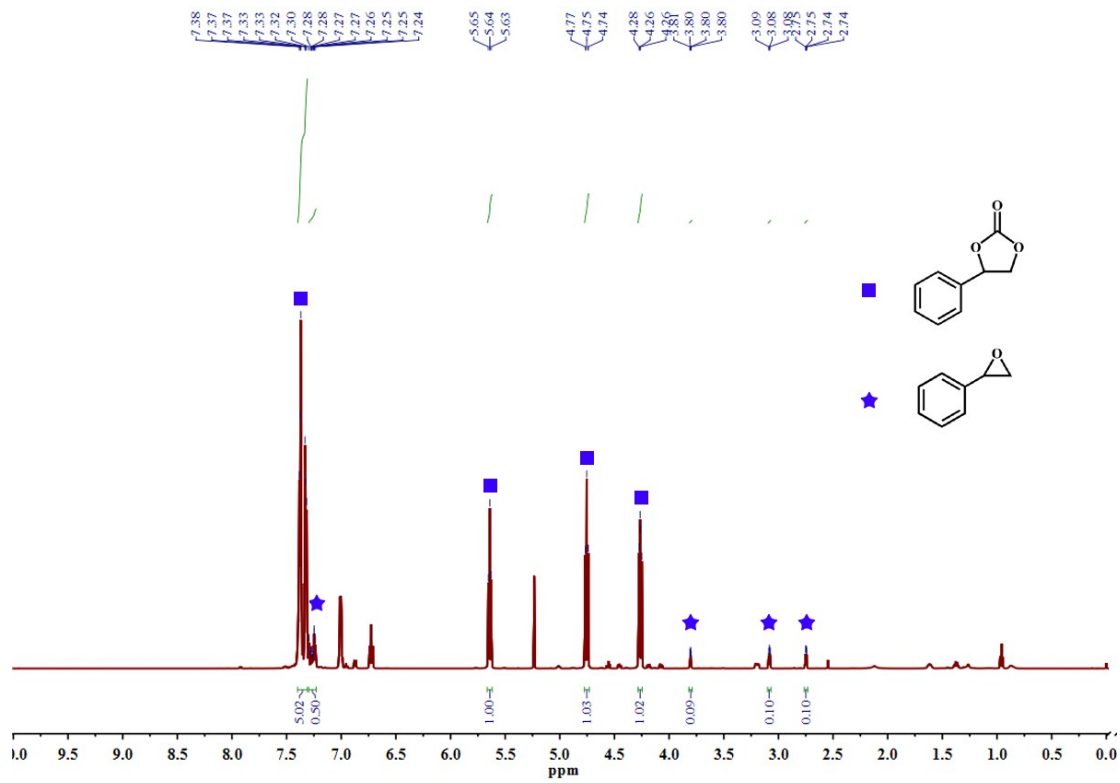
Fig. S11 GC of cycloaddition of CO₂ to epichlorohydrin using catalyst **2** and *n*-Bu₄NBr as co-catalyst for (a) 0.5 hour, (b) 1 hour, (c) 1.5 hours and (d) after removing catalysts at 1 atm.



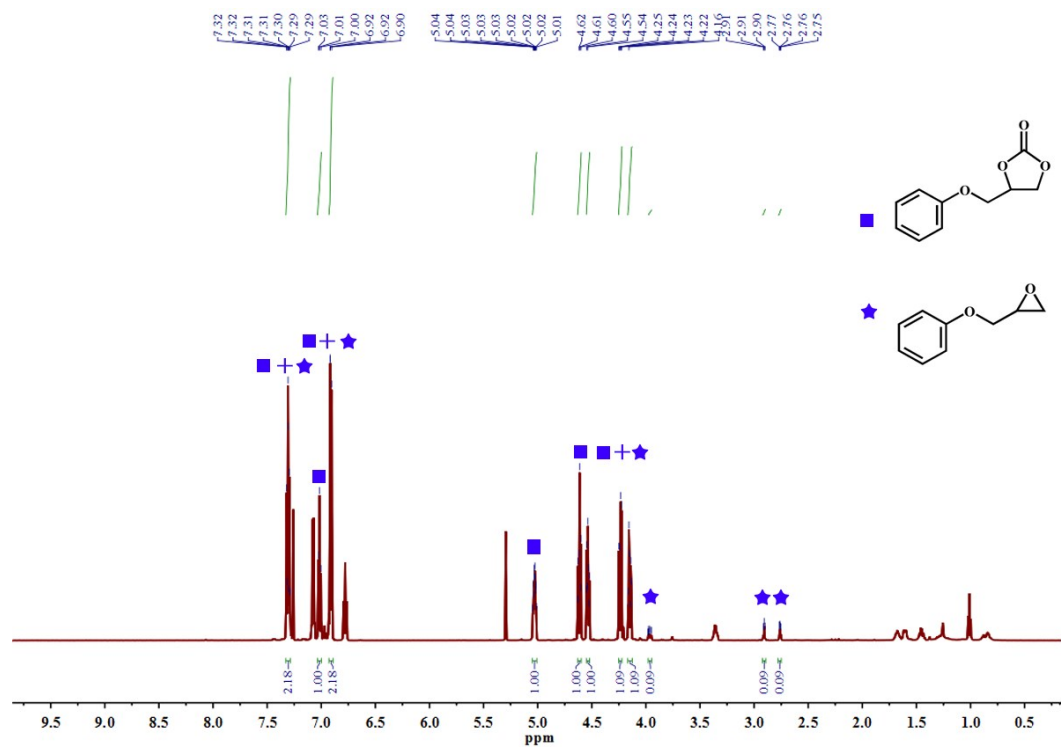
(a)



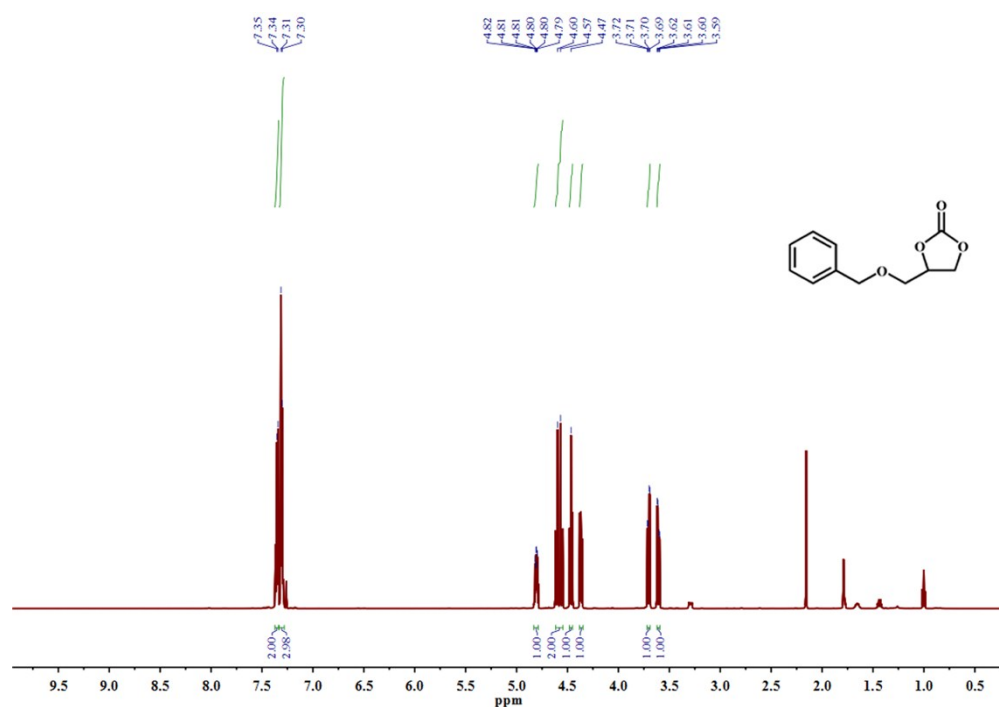
(b)



(c)



(d)



(e)

Fig. S12 (a) ¹H NMR spectrum of the product 4-chloromethyl-1,3-dioxolan-2-one achieved from the cycloaddition of CO₂ to epichlorohydrin.

(b) ¹H NMR spectrum of the product 4-butyl-1,3-dioxolan-2-one achieved from the cycloaddition of CO₂ to 1,2-epoxyhexane.

(c) ¹H NMR spectrum of 1,2-epoxyethylbenzene and its corresponding reaction mixture. ¹H NMR (500 MHz, CDCl₃) for 4-phenyl-1,3-dioxolan-2-one.

(d) ¹H NMR spectrum of glycidylphenylether and its corresponding reaction mixture. ¹H NMR (500 MHz, CDCl₃) for 4-(phenoxyethyl)-1,3-dioxolan-2-one.

(e) ¹H NMR spectrum of the product 4-(phenylmethoxymethyl)-1,3-dioxolan-2-one achieved from the cycloaddition of CO₂ to glycidylbenzylether.

The signals at 0.5-2.0 ppm and 5.3 ppm are caused by the impurities in CDCl₃ during the ¹H NMR testing.

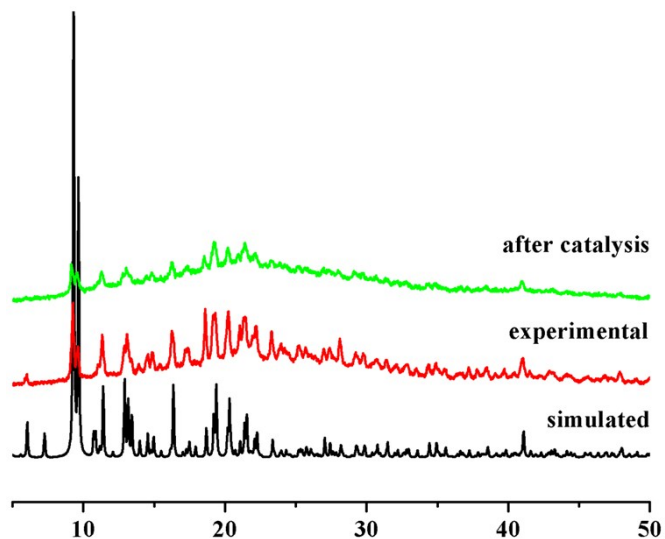


Fig. S12 PXRd patterns of the simulated (black), the experimental (red) and after 4 cycles cycloaddition reaction catalyzed by **2** (green).

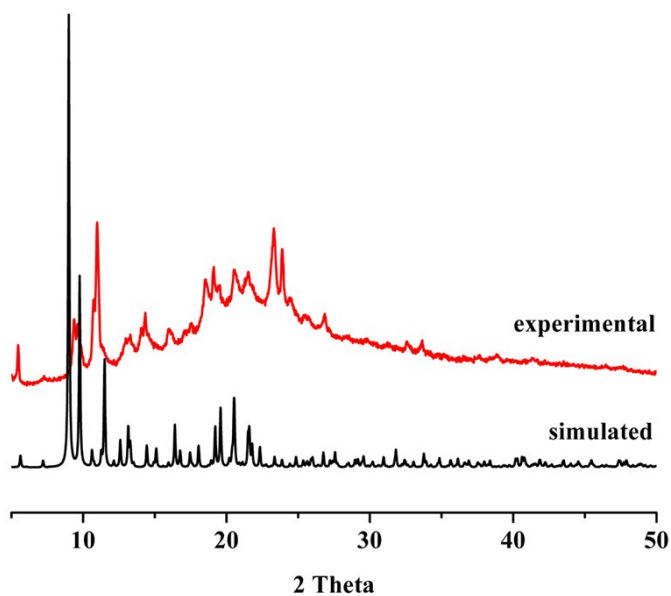


Fig. S13 PXRd patterns of the simulated (black) and the experimental (red) of **1a**.

Table S1 Crystal Data and Structure Refinements.

	1	2	1a
Formula	C ₇₈ H ₈₅ O ₂₅ N ₁₃ Cd ₃	C ₈₄ H ₉₅ O ₂₈ N ₁₅ Zn ₃	C ₈₁ H ₇₈ O ₁₈ N ₁₂ Cd ₃
<i>Mr</i>	1941.78	1958.85	1844.75
Crystal system	hexagonal	hexagonal	hexagonal
space group	<i>P</i> -62 <i>c</i>	<i>P</i> -62 <i>c</i>	<i>P</i> -62 <i>c</i>
<i>a</i> /Å	18.3047(6)	19.4560(11)	18.1130(5)

$b/\text{\AA}$	18.3047(6)	19.4560(11)	18.1130(5)
$c/\text{\AA}$	37.9711(15)	37.381(3)	39.2720(15)
$\alpha/^\circ$	90	90	90
$\beta/^\circ$	90	90	90
$\gamma/^\circ$	120	120	120
$V/\text{\AA}^3$	11018.2(8)	12254.3(16)	11158.2(6)
Z	4	4	4
D_c (g/cm ³)	1.171	1.062	1.098
$F(000)$	3952	4072	3744
GOF on F^2	0.848	0.959	1.100
R_{1a} [$I > 2\sigma(I)$]	0.0494	0.0583	0.0688
wR_2^b (all data)	0.1375	0.1725	0.2043
$R(\text{int})$	0.0678	0.0757	0.0543

$$^aR_1 = \frac{\sum ||F_o| - |F_c||}{\sum |F_o|}. \quad ^b wR_2 = \left\{ \frac{\sum [w(F_o^2 - F_c^2)^2]}{\sum w(F_o^2)^2} \right\}^{1/2}.$$

Table S2 Selected Bond Distances (Å) and Angles (°) for **1**, **2** and **1a**.

1

Cd(1)-N(1)	2.233(7)	Cd(1)-N(3)	2.248(7)
Cd(1)-O(3)	2.262(5)	Cd(1)-O(1)	2.308(5)
Cd(1)-O(2)	2.414(5)	Cd(1)-O(4)	2.460(5)
N(1)-Cd(1)-N(3)	97.9(3)	N(1)-Cd(1)-O(3)	125.5(2)
N(3)-Cd(1)-O(3)	116.8(2)	N(1)-Cd(1)-O(1)	88.3(2)
N(3)-Cd(1)-O(1)	135.0(2)	O(3)-Cd(1)-O(1)	93.9(2)
N(1)-Cd(1)-O(2)	123.8(2)	N(3)-Cd(1)-O(2)	87.2(2)
O(3)-Cd(1)-O(2)	99.7(2)	O(1)-Cd(1)-O(2)	53.98(17)
N(1)-Cd(1)-O(4)	87.3(2)	N(3)-Cd(1)-O(4)	90.2(2)
O(3)-Cd(1)-O(4)	54.35(18)	O(1)-Cd(1)-O(4)	134.8(2)
O(2)-Cd(1)-O(4)	148.77(18)		

2

Zn(1)-O(3)	1.941(5)	Zn(1)-O(6)	1.997(19)
Zn(1)-N(4)	1.978(9)	Zn(1)-N(2)	2.022(9)
O(3)-Zn(1)-O(6)	106.5(5)	O(3)-Zn(1)-N(4)	113.8(3)

O(6)-Zn(1)-N(4)	111.5(7)	O(3)-Zn(1)-N(2)	115.8(3)
O(6)-Zn(1)-N(2)	102.1(8)	N(4)-Zn(1)-N(2)	106.6(3)
1a			
Cd(1)-O(4)	2.201(8)	Cd(1)-N(4)	2.219(11)
Cd(1)-N(1)	2.238(12)	Cd(1)-O(5)	2.262(9)
Cd(1)-O(6)	2.482(9)	Cd(1)-O(3)	2.597(7)
O(4)-Cd(1)-N(4)	114.2(4)	O(4)-Cd(1)-N(1)	120.1(3)
N(4)-Cd(1)-N(1)	101.4(5)	O(4)-Cd(1)-O(5)	96.5(3)
N(4)-Cd(1)-O(5)	136.8(4)	N(1)-Cd(1)-O(5)	87.1(4)
O(4)-Cd(1)-O(6)	108.1(3)	N(4)-Cd(1)-O(6)	86.5(4)
N(1)-Cd(1)-O(6)	121.1(4)	O(5)-Cd(1)-O(6)	54.2(3)
O(4)-Cd(1)-O(3)	53.6(3)	N(4)-Cd(1)-O(3)	85.2(4)
N(1)-Cd(1)-O(3)	85.6(3)	O(5)-Cd(1)-O(3)	138.0(3)
O(6)-Cd(1)-O(3)	153.2(3)		